

Journal of Atmospheric and Solar-Terrestrial Physics
Low latitude geomagnetic response associated with intense geomagnetic storms:
regional space weather in Mexico
--Manuscript Draft--

Manuscript Number:	JASTP-D-23-00207
Article Type:	VSI:COLAGE's Special Edition
Section/Category:	Space weather
Keywords:	Space Weather Geomagnetic Storms Regional Response Ionospheric Currents
Corresponding Author:	Carlos Isaac Castellanos-Velazco, M.S Consorcio Universidad Nacional Autonoma de Mexico Morelia, Morelia MEXICO
First Author:	Carlos Isaac Castellanos-Velazco, M.S
Order of Authors:	Carlos Isaac Castellanos-Velazco, M.S Pedro Corona-Romero, Ph. D. Juan Américo González-Esparza, Ph. D Ana Luz Caccavari-Garza, Ph. D Maria Alexandra Sergeeva, Ph. D
Manuscript Region of Origin:	North America
Abstract:	<p>Highlights</p> <p>Low latitude geomagnetic response associated with intense geomagnetic storms: regional space weather in Mexico Castellanos-Velazco, C. I., Corona-Romero, P., González-Esparza, J. A., Caccavari-Garza, A. L., Sergeeva, M. A.</p> <ul style="list-style-type: none">• Research of space weather activity over center of Mexico• Analysis of differences in local and planetary geomagnetic responses during a geomagnetic storm.• Study of ionospheric currents related to geomagnetic storms, known to drive local geomagnetic fluctuations.

Highlights

Low latitude geomagnetic response associated with intense geomagnetic storms: regional space weather in Mexico

Castellanos-Velazco, C. I., Corona-Romero, P., González-Esparza, J. A., Caccavari-Garza, A. L., Sergeeva, M. A.

- Research of space weather activity over center of Mexico
- Analysis of differences in local and planetary geomagnetic responses during a geomagnetic storm.
- Study of ionospheric currents related to geomagnetic storms, known to drive local geomagnetic fluctuations.

Highlights

- Research of space weather activity over center of Mexico.
- Analysis of differences in local and planetary geomagnetic responses during a geomagnetic storm.
- Study of ionospheric currents related to geomagnetic storms, known to drive local geomagnetic fluctuations.

Abstract

In this paper, we present our first steps towards the monitoring, in near real-time, of the geomagnetic activity in the continental territory of Mexico by the Space Weather National Laboratory (LANCE) via the Geomagnetic Stations Network of Mexico (REGMEX). REGMEX aims to monitor the geomagnetic field at five different sites in near real-time. The collected data will be processed to promptly compute and publish Mexico's regional geomagnetic-activity indices (ΔH and K). Currently, Mexico lacks facilities to simultaneously monitor geomagnetic activity in real-time across its territory. This work shows the way in which LANCE endeavors to solve the lack of such geomagnetic data by presenting the REGMEX's development plan and its current development status. In addition, we show geomagnetic storms as registered by our available regional geomagnetic indices and compare those records with their planetary counterparts.

Low latitude geomagnetic response associated with intense geomagnetic storms: regional space weather in Mexico

Castellanos-Velazco, C. I.^a, Corona-Romero, P.^b, González-Esparza, J. A.^b, Caccavari-Garza, A. L.^c and Sergeeva, M. A.^{b,**}

^aPrograma de Posgrado en ciencias de la Tierra, , Instituto de Geofísica Unidad Michoacán, Universidad Nacional Autónoma de México, , Morelia, 58341, Michoacán, México

^bInvestigadores por México-CONACYT, Servicio de Clima Espacial México, Laboratorio Nacional de Clima Espacial, Instituto de Geofísica Unidad Michoacán, Universidad Nacional Autónoma de México, , Morelia, 58089, Michoacán, México

^cInvestigadores por México-CONACYT, Servicio Magnético, Instituto de Geofísica, Universidad Nacional Autónoma de México, , Mexico city, 04150, México

ARTICLE INFO

Keywords:

Space Weather
Geomagnetic Storms
Regional Response
Ionospheric Currents
Disturbed Dynamo
Disturbed Polar Current 2

ABSTRACT

In this work we studied the regional manifestations of space weather at central Mexico through isolate the local geomagnetic response from its planetary counterpart. In order to do so, we analyzed 20 intense geomagnetic storms by identifying the ionospheric contribution in their regional geomagnetic data as registered at central Mexico. Our analysis indicated that local geomagnetic response is mainly driven by ionospheric disturbances. We also found that the *disturbed polar current number 2* and the *disturbed dynamo current* are particularly relevant for the regional geomagnetic response. Finally, we showed that regional geomagnetic activity can be approximated by the combined effects of the geomagnetic planetary response and the magnetic perturbations induced by the commented ionospheric currents.

1. Introduction

Geomagnetic storms (GS) are relevant subjects for space weather, since they can negatively affect facilities, products and services related to communications, navigation systems and energy supply (Schrijver, 2015). GSs are related to solar activity and mainly imply a temporal weakening of the Earth's magnetic field (EMF), among other phenomena (Gonzalez et al., 1994). A GS occurs when the magnetosphere's current system is perturbed by solar wind material that penetrated into the EMF through magnetic reconnection between the interplanetary magnetic field (IMF) and the EMF (Baumjohann and Treumann, 1999; C.T Russell, 2016).

Generally, GSs are identified through geomagnetic indices, that also allow to quantify their magnitudes. There are many types of geomagnetic indices, and each one is designed to register particular aspects of a geomagnetic perturbation. For the case of middle and low latitudes, the most frequently used are the planetary K (K_p) and the disturbance storm time (Dst) indices; since in those regions a GS can be clearly registered on the EMF's horizontal component (H) which is the input data to compute these indices. The K_p index quantifies the three-hourly maximum variation on H observed at mid-latitudes. On the other hand, the Dst index is an hourly average of perturbations on H as measured around the Earth's magnetic equator. The planetary indices

(K_p and Dst) have regional counterparts that used regional data instead of planetary averages. (Mayaud, 1980)

GSs are planetary phenomena, however, the way they manifest at regional scale may vary for different locations. This could be caused by the heterogeneity of the Earth, the asymmetries in magnetospheric and ionospheric currents, as well as the way the magnetosphere and ionosphere interact in each region. Thus, geomagnetic latitude, local time or even the year's season may affect the way a GS manifests at regional scale, which in turn also may determine its effects on the technologies our societies depend on. In consequence, overlooking the regional factor in GSs may lead to some uncertainties or misinterpretation in the attempt of understand and address the possible effects related to GS events (Pirjola, 2000; Bailey et al., 2017; Vodyannikov et al., 2006; da Silva Barbosa et al., 2015).

Space weather studies for regions within middle and low geomagnetic-latitudes has became of more interest in recent decades. For example, Hejda and Bochníček (2005); da Silva Barbosa et al. (2015) and Bailey et al. (2017) show the relevance of studying these phenomena for mid and low latitudes. In the particular case of Mexico, which is a mid and low latitudes country, there were attempts to do regional ionospheric and geomagnetic studies (Pérez-Enríquez and Kotsarenko, 2003; Gonzalez-Esparza et al., 2005; Rodriguez-Martinez et al., 2011; Carrillo-Vargas et al., 2012; Rodriguez-Martinez et al., 2011; López-Montes et al., 2012; Rodriguez-Martinez et al., 2014; Merline Matamba et al., 2016; Martínez-Bretón L. et al., 2016). Nevertheless, the systematic study and monitoring of regional space weather formally began by 2014 when the Mexican Space Weather Service (SCIESMEX), Geophysics Institute (IGF) at National and Autonomous University of Mexico (UNAM)

*Corresponding author

✉ ccastellanos@igeofisica.unam.mx (C.C. I.);

p.coronaromero@igeofisica.unam.mx (C. P.); americoo@igeofisica.unam.mx (G.J. A.)

ORCID(s): 0000-0001-8818-5318 (C.C. I.); 0000-0002-2573-2967 (C. P.); 0000-0003-4774-1829 (G.J. A.)

began operations. Subsequently, by 2016, there was a significant increment in infrastructure and technologies dedicated to study and monitoring regional space weather with the beginning of operations of the Mexican Space Weather National Laboratory (LANCE), at IGF-UNAM. (Gonzalez-Esparza et al., 2017)

By combining efforts and resources, the couple SCI-ESMEX/LANCE has made possible to identify that regional geomagnetic response can potentially be driven by ionospheric disturbances during GS periods (see Romero-Hernandez et al., 2017; Sergeeva et al., 2017, 2019; Corona-Romero et al., 2018, 2017). This result is in agreement with other mid and low latitudes studies, since it is known that for low and middle latitudes there are two main sources of geomagnetic fluctuations driven(induced) by ionospheric currents: the *disturbed polar current number 2* (DP2) (Nishida, 1968a,b, 1966) and the *disturbed dynamo current* (Ddyn) (Blanc and Richmond, 1980).

On one hand, the DP2 current is associated with electric fields induced during the magnetic reconnection between the interplanetary magnetic field and the EMF. Those electric fields are then convected along the Birkeland currents (Wei et al., 2015; Kikuchi and Hashimoto, 2016) up to reaching high ionospheric latitudes, where it drives a pattern of two ionospheric convective twin cells known as DP2 currents. The charged particles in those cells are drift by the centrifuge and curvature effects of the EMF, condition that induces a polarized electric field (Heppner, 1972b,a; Bobova et al., 1985; Blanc and Caudal, 1985; Denisenko et al., 1992). During the main phase of a GS, such a polarized electric field, together with the DP2 current, may extend beyond high latitudes reaching mid, and even low, latitudes (Nishida, 1966, 1968a; Obayashi and Nishida, 1968).

On the other hand, the Ddyn currents are enhances of the polar ionospheric currents due to the precipitation of energetic particles occurring during the main phase of a GS. The resulting Joule heating in the thermosphere generates circulation of neutral winds and charged particles in equatorward direction. The Coriolis force cause a westward change of direction on these polar-equatorial flows, at mid and low latitudes (Blanc and Richmond, 1980; Le Huy and Amory-Mazaudier, 2005; Zaka et al., 2009). During this process there is an induction of the Pedersen currents equatorward and accumulation of charged particles along the dip equator. This accumulation drives electric fields poleward and a second Pedersen current in the same direction which is opposed to the first one. As consequence, Hall currents are driven eastward at mid latitudes ($\sim 45^\circ$), currents that are interrupted at terminators (Blanc and Richmond, 1980). Then, currents present a divergence with closure at adjacent latitudes, giving place to two vortexes shaped currents called *Disturbed dynamo currents*.

Since the Ddyn and DP2 ionospheric currents may affect the geomagnetic response at mid and low latitudes, we wonder if these ionospheric currents could be the mechanisms that link the regional geomagnetic response with local ionospheric perturbations in central Mexico. Answering that

is our main motivation in this work, along which we first identify differences between regional and planetary geomagnetic activities, with the purpose of isolate regional geomagnetic response during GSs. Once the regional response is isolated, we proceed to search for evidence of Ddyn and DP2 mechanisms as sources of such regional geomagnetic response. In order to do so, we identify their signatures in magnetic registers. Subsequently, we validate our results by comparing planetary and regional indices of geomagnetic activity and discuss our concluding remarks.

2. Methodology

2.1. Local geomagnetic response

In order to identify regional geomagnetic response we analyzed 20 geomagnetic storms (GS) events. Our selected events occurred between 2003 to 2018, period of time that covers the descending phase of solar cycle 23 and most of solar cycle 24. The events were registered by the Geomagnetic Observatory of Teoloyucan (TEO), located at 27.84°N 28.41°W . TEO is operated by the Magnetic Service of the Geophysics Institute at National and Autonomous University if Mexico. Our selected events share values of local K index (K_{TEO}) above 6+. They also have values of ΔH_{TEO} (regional counterpart of Dst index) less than -120 nT. Table 1 shows all the analyzed events.

We assume that significant differences between regional and planetary geomagnetic indices should be provoked by local geomagnetic response. Thus, in order to identify such differences we directly compare Dst and ΔH_{TEO} for our studied events. Figure 1 shows a dispersion plot that compares the regional response (vertical axis) with its planetary counterpart (horizontal axis). In the figure we observe two well differentiated tendencies in data distribution: The first one ($Dst \geq \lambda 100$ nT) where the data points closely follow the identity (solid black line), and the second one (green-shadowed region) where the data dispersion detached from the identity ($Dst < \lambda 100$ nT). This appreciation is agreement with the correlation indices of each region, which gives $R^2 = 0.77$ for the first one, and $R^2 = 0.42$ for the latter.

Figure 1 shows, in the case of our analyzed events, that planetary and regional geomagnetic indices may significantly differ each other. Which in turn suggests the presence of some kind of local (ionospheric) mechanisms with the capability to deviate the regional value of geomagnetic field from its planetary counterpart. Hence, we need to identify in the regional geomagnetic registers the signatures for the magnetic contribution cause by those ionospheric mechanisms (Le Huy and Amory-Mazaudier, 2005; Zaka et al., 2009; Amory-Mazaudier et al., 2017; Younas et al., 2020). Now we proceed to identify such mechanisms.

2.2. Geomagnetic signatures of local ionospheric currents

The local values of EMF are result from the contribution of many sources (Rishbeth and Garriott, 1969; Knecht and B.M, 1985; Gjerloev, 2012; van de Kamp, 2013). In the

Table 1

Study cases: Event number, GS main phase beginning date, minimum(maximum) values reached during the events for Dst(K_p) and ΔH_{TEO} (K_{TEO}) geomagnetic indices, respectively.

Event #	Beginning of main phase	^a Dst minimum [nT]	^b ΔH minimum [nT]	^a K_p maximum	^b K_{TEO} maximum
1	2003/05/29	-144	-190	8+	9
2	2003/10/14	-85	-126	7+	7-
3	2003/11/20	-422	-441	9-	9
4	2004/07/22	-170	-167	9-	8+
5	2004/08/30	-129	-154	7	7-
6	2004/11/08	-374	-398	9-	9
7	2005/05/15	-247	-206	8+	7
8	2005/06/12	-106	-120	7+	6+
9	2005/08/24	-184	-138	9-	9-
10	2005/08/31	-122	-125	7	6+
11	2006/08/19	-79	-131	6	7-
12	2006/12/14	-162	-247	8+	9
13	2015/03/15	-222	-282	8	8-
14	2015/10/07	-124	-143	7+	7+
15	2015/12/20	-155	-189	7-	7
16	2016/03/06	-98	-120	6	7
17	2016/10/13	-104	-128	6+	6+
18	2017/05/27	-125	145	7	8
19	2017/09/07	-124	-170	8+	8+
20	2018/09/25	-175	-176	7+	7-

Comments for the Table.

^a Dst and K_p were obtained from the International Service of geomagnetic Indices (ISGI).

^b Regional geomagnetic indices ΔH_{TEO} and K_{TEO} were computed by the Space Weather National Laboratory, using TEO geomagnetic registers.

particular case of the horizontal component (H) of local EMF, we can express it as:

$$H = B_{SQ} + H_0 + D_M + D_I, \quad (1)$$

where B_{SQ} is the diurnal variation obtained from the local quiet days (van de Kamp, 2013); H_0 is the variation day to day (Gjerloev, 2012). The last two terms are irregular magnetic variations related to geomagnetic activity Le Huy and Amory-Mazaudier (2005); Zaka et al. (2009): with D_M being the contribution from (planetary scale) magnetospheric currents, and D_I is the magnetic contribution driven by ionospheric perturbations. Furthermore, in the case of mid and low latitudes, $Dst \cdot \cos(\lambda)$ can approximate D_M , with λ being the geomagnetic latitude (Amory-Mazaudier et al., 2017). Such approximation transforms Equation 1 into:

$$D_I \approx H - (B_{SQ} + H_0 + Dst \cdot \cos(\lambda)). \quad (2)$$

In addition, D_I can be expressed as:

$$D_I = DP2 + Ddyn + D_{others}, \quad (3)$$

with D_{others} are ionospheric perturbations different from $DP2$ and $Ddyn$.

In order to isolate the magnetic signatures of $DP2$ and $Ddyn$ in Equations (2) and (3), we shall apply frequency filters to analyze D_I (Younas et al., 2020). These filters should rely on the range of frequencies (periods) in which each current induce magnetic fluctuations on the local EMF. On one hand, it is known that the magnetic fluctuations induced by $Ddyn$ oscillates with main periods of approximately 24 h, whereas the oscillation periods of those fluctuations induced by $DP2$ are less or equal than 4 h Blanc and Richmond (1980); Zaka et al. (2009). In consequence, those filters need to be a pass-band filter for the case of $DP2$ and high-pass filter for $Ddyn$ (Nishida, 1968b; Blanc and Richmond, 1980).

3. Analysis and results

3.1. Local ionospheric disturbances and induced magnetic fluctuations

In this section we present our analysis process through analyzing event 13. The panel (a) of Figure 2 shows the the profiles of Dst (black) and ΔH (green) indices during the GS associated with event 13 (see Table 1). In the panel we observe that both indices are *quiet* up to the start of the GS's main phase signed out by a vertical dotted-line. The main phase lasts approximately one day reaching a minima

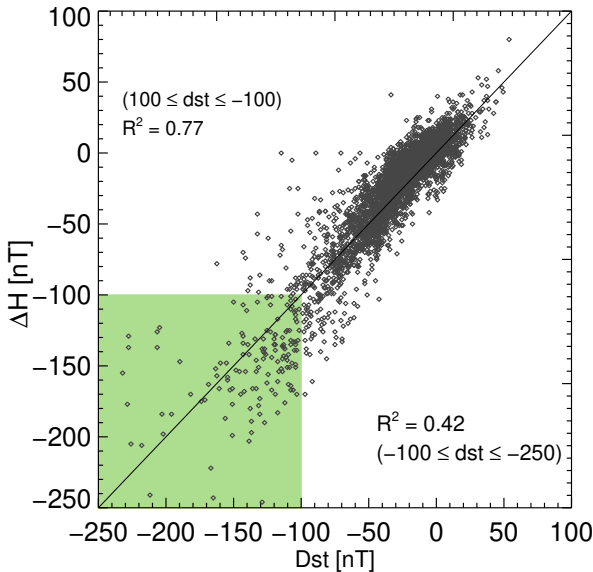


Figure 1: Dispersion plot of ΔH (vertical axis) with respect to Dst (horizontal axis) for all GS events. The green region represents a -100 nT threshold in which it was computed a second R^2 .

of $Dst \sim -300$ nT, whereas the recovering phase extends almost three days.

In the panel (b) of Figure 2, we appreciate the resulting profile of D_I (Equation (2)), which we computed using the TEO's registers and the Dst reported data. Subsequently, we proceed to construct a power spectrum for our computed profile of D_I , which we show in panel (d) of Figure 2. In the power spectrum we highlight, by a yellow shadowing, the range of periods(frequencies) consistent with $DP2$ and $Ddyn$. In the panel we identify $Ddyn$'s range by setting the main period and searching potency peaks within the range of possible harmonics. It is important to remark that, due to our study cases might be potentially different each other, the filtering ranges might slightly variate from case to case.

In the Figure 2(c) we present the profiles of the induced magnetic perturbations caused by $DP2$ (solid red line) and $Ddyn$ (solid black line). These profiles are constructed departing from the frequencies identified through the filtering process commented in the previous paragraph. We note that the enhancements of the induced effects of $Ddyn$ and $DP2$ simultaneously occurs with an increase in the total electron content over central Mexico, as the panel (e) of Figure 2 shows.

We applied the procedure presented in this section to all our study cases. The Figures 6 and 7 in the Appendix show the computed D_I and the resulting profiles of $DP2$ and $Ddyn$, for each event in Table 1. We remark the uniqueness of each event, that is clear in the D_I profiles and its associated magnetic perturbations induced by $DP2$ and $Ddyn$ currents.

From Figures 6 and 7 we note that generally the amplitude of the magnetic oscillations induced by $Ddyn$ are more intense than those induced by $DP2$. This suggest

that, in most of cases, $Ddyn$'s induced magnetic effects are dominant on the local EMF. Although there are events for which both effects show similar intensities. We think in two possibilities to explain that: The first is the process that triggering the GS its self, *i.e.* the solar activity event and its magnetic reconnection with the EMF. This may affect the evolution on the ionospheric response, and directly modifying the evolution of $DP2$ and $Ddyn$ currents. Secondly, we have to consider that our data is sampled in hourly resolution. In this case, data sampling represents an important limitation since $DP2$ magnetic fluctuations, as mentioned in Nishida (1968b), may have periods of less than an hour, or even of tens of minutes. In this scenario, we possibly missed part of $DP2$ fluctuations during our analysis. This could be solved, in principle, by using $Sym - H$ index rather than Dst , task which exploration we consider our future work.

3.2. Validation of $DP2$ and $Ddyn$ magnetic signatures

In Section 2.1 we were able to identify significant differences between the planetary and regional geomagnetic activity. Condition that we associated to regional geomagnetic response. Subsequently, in Section 3.1, we identified the tentative geomagnetic mechanisms for that regional geomagnetic response. Such mechanism are the $Ddyn$ and $DP2$ ionospheric currents, whose effects were reconstructed by a periods (frequencies) filtering process. We also learned that those effects are systematically associated with local perturbations on TEC. Now, we require to validate our results.

In order to validate our previous results, first we approximate the regional geomagnetic index ΔH , which can be defined as:

$$\Delta H = H - (B_{SQ} + H_0), \quad (4)$$

through Dst and the resulting profiles of $DP2$ and $Ddyn$. Thus, by manipulating Equations (2), (3) and (4) we obtain that:

$$\Delta H \approx Dst \cos(\lambda) + DP2 + Ddyn. \quad (5)$$

For simplicity, we call Dst_λ the combined effects of $Dst \cos(\lambda)$, $DP2$ and $Ddyn$. Hence, our first step for validation is to corroborate that our computed value of Dst_λ approximates ΔH . In addition, we can also used Dst_λ and the values of K_p to approximate the local value of K .

The results of the validation process commented on before applied on event 13 are shown by Figure 3. The upper panel of Figure 3 compares the profiles of ΔH (black), Dst (green) and Dst_λ (red). In the panel we note that Dst_λ is systematically closer to ΔH than Dst . This condition holds during the main and recovering phases of the GS. Additionally, in the bottom panel of Figure 3 it is clear that the planetary (green) and local (black) values of K index differ each other. Nevertheless, when we combine K_p with the values of Dst_λ , as uncertainty bars, we appreciate that local K profile, in general, falls inside those bars.

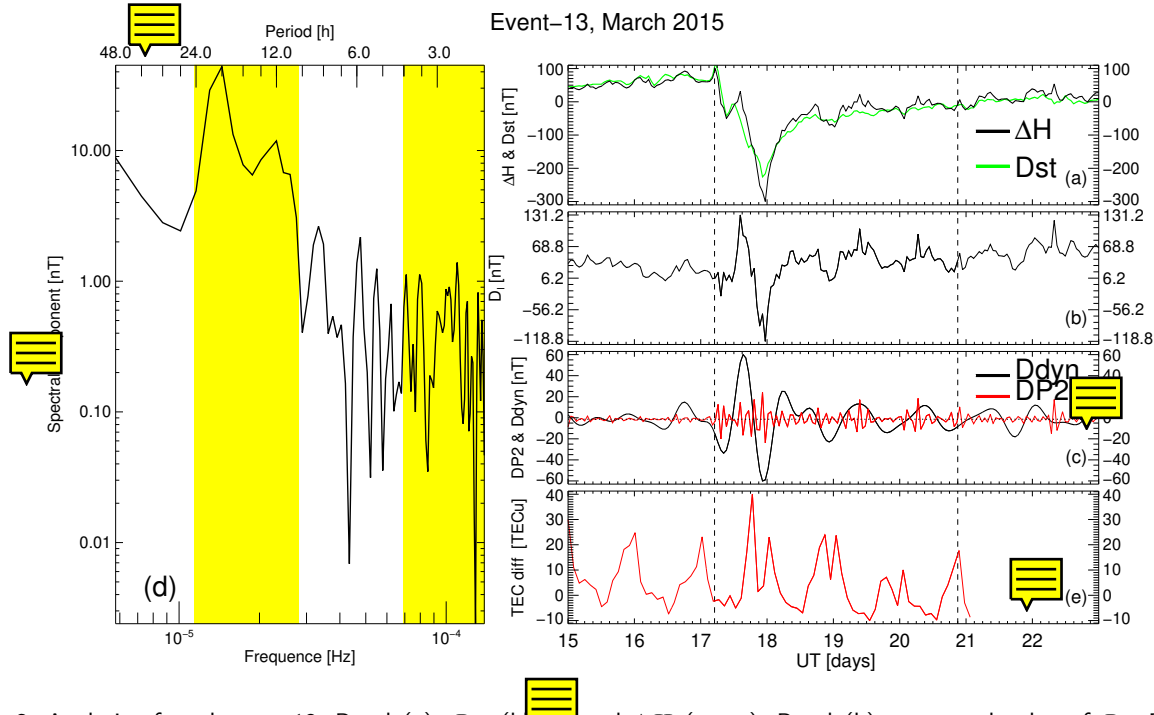


Figure 2: Analysis of study case 13. Panel (a): Dst (black) and ΔH (green). Panel (b): computed value of D_I . Panel (c): Reconstructed profiles of the induced geomagnetic effects of D_{dyn} (black line) and $DP2$ (red line). Panel (d): Power spectrum of D_I . Panel (e): Measured total electron content (TEC) over center of Mexico. Dotted vertical lines mark out the start (left) and end (right) of GS. Yellow shadowing regions in panel (d) highlight the bandwidths associated to D_{dyn} (25h - 10 h) and $DP2$ (less than 4.5 h) filters.

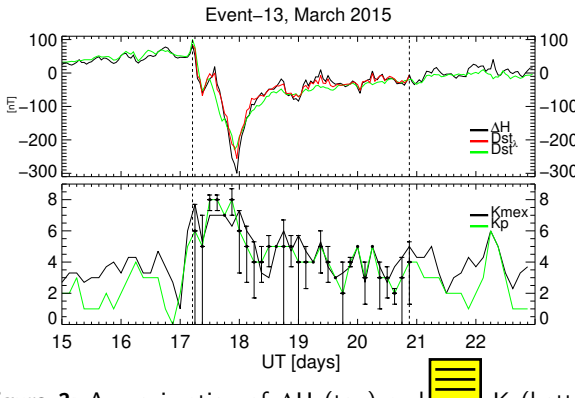


Figure 3: Approximation of ΔH (top) and K_p (bottom) geomagnetic indices. The green solid lines represent planetary indices and black solid lines represents local geomagnetic indices. The approximated ΔH index is represented by the red line while the error bars represent an approximation range for K_{mex} index.

This process was repeated with all our study cases. The Figures 8 and 9 show the results of our validation exercise. In all the cases, we found that Dst_λ consistently approximates ΔH . We also found that K_p with the combined effects of Dst_λ was able to enclose the regional K values.

Now, in addition to our previous qualitative comparison; we proceed with a quantitative exploration. For this purpose we compute the average absolute difference between

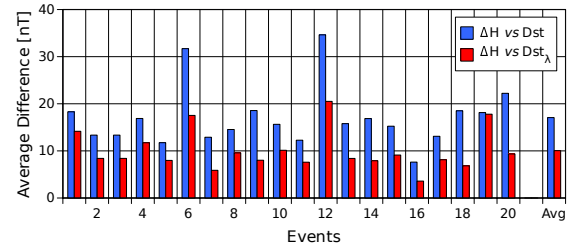


Figure 4: Average error (Top) measured in nT between ΔH vs Dst and ΔH vs Dst_λ . Error difference (bottom) between the two cases above.

the pairs $\Delta H-Dst$ and $\Delta H-Dst_\lambda$ for our study cases. The results for this exploration are shown by Figure 4. In the figure we observe a histogram with the average difference between $\Delta H-Dst$ (blue bars) and $\Delta H-Dst_\lambda$ (red bars). We note that average difference associated with Dst_λ is systematically lesser than that associated with Dst . This result indicates that the effects of magnetic perturbations consistent with those provoked by $DP2$ and D_{dyn} are relevant for regional geomagnetic response.

Finally, our third and last step for our validation process is to remake the dispersion plot of Figure 1, but using Dst_λ data instead of Dst 's. Figure 5 shows the new dispersion plot where we can appreciate, in contrast with Figure 1, that data points (open diamonds) closely follow the identity (solid black line). Furthermore, when we compute the correlation

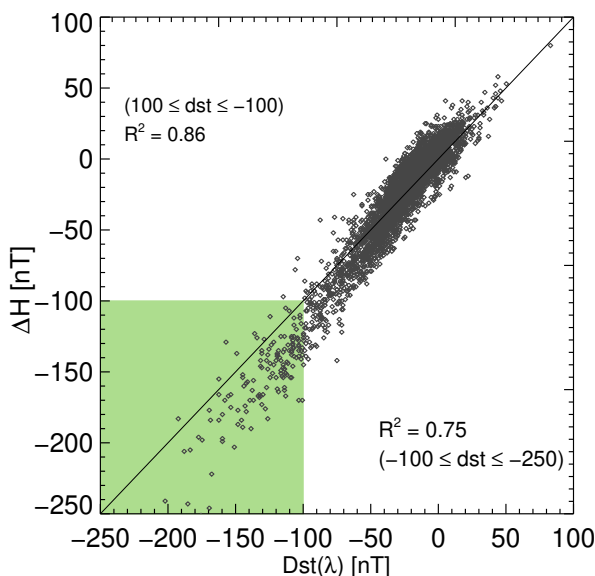


Figure 5: Dispersion plot of ΔH (vertical axis) with respect to $Dst(\lambda)$ (horizontal axis) for all GS events. The green region represents a -100 nT threshold in which it was computed a second R^2 .

indices we obtain note that R^2 grew from 0.77 up to 0.86 for the range of $Dst \geq -100$ nT. In addition, for the case of $Dst < -100$ nT, $R^2 = 0.75$ which is significant increment from the value originally associated to Dst ($R^2 = 0.42$).

Our validation process proved that the magnetic perturbations tentatively induced by $DP2$ and $Ddyn$ ionospheric currents, when combined with planetary indices, allowed to qualitatively approximate the regional geomagnetic activity. We also proved that regional geomagnetic response, as registered by ΔH , can be quantitatively expressed by the planetary response (Dst) combined with the geomagnetic effects of the already commented ionospheric currents. Finally, when including the magnetic effects induced by $DP2$ and $Ddyn$ into the planetary response, the dispersion between regional and planetary data substantially decreased.

4. Concluding remarks

In this work we studied the regional manifestations of space weather. We focused on the differences between planetary and local geomagnetic responses during periods of strong geomagnetic storms (GS) at center of Mexico. We also investigated the possible sources for such differences in the geomagnetic response. In order to do so, we used the geomagnetic registers from the Teoloyucan Magnetic Observatory (TEO), located at north of Mexico City. We also use data sets from the Dst and K_p planetary indices, as well as the regional geomagnetic index ΔH and the total electron content delivered by the Mexican Space Weather National Laboratory.

We selected 20 GS as study cases for this work (see Table 1). For all our study cases we identified evidence for the presence of relevant regional geomagnetic response

through a dispersion plot (see Figure 1). In this regard, we found that in the range of $Dst < -100$ nT there is a tendency for the regional geomagnetic index to deviate from the planetary one. We assumed this as an evidence for regional geomagnetic response.

Subsequently, we isolated the geomagnetic effects due to ionospheric processes (D_I) from the regional (TEO) geomagnetic registers. Next, we applied filters on D_I with the purpose of identify the magnetic perturbations consistent with those induce by $Ddyn$ and $DP2$ currents. We also verified that intensification of the resulting $Ddyn$ and $DP2$ profiles simultaneously occurred during TEC perturbations (see discussion of Figure 2). In consequence, we were able to reconstruct the regional geomagnetic response consistent with those induced by $Ddyn$ and $DP2$ currents.

Afterwards, we validate our computed geomagnetic contribution due to $Ddyn$ and $DP2$ currents. First, we approximate the regional K and ΔH indices by combining the planetary K_p and Dst indices with the regional geomagnetic effects of $Ddyn$ and $DP2$. Secondly, we computed the differences between ΔH and Dst with and without the regional ionospheric effects. Finally, we analyzed the dispersion between ΔH and Dst combined with the effects of $Ddyn$ and $DP2$. For all the cases, we found that regional geomagnetic response is qualitatively and quantitatively approximated by the geomagnetic planetary response combined with the geomagnetic perturbations induced by the $Ddyn$ and $DP2$ ionospheric currents.

Finally, in this work we focus on regional space weather. We identified evidence of regional geomagnetic response that is significantly different from its planetary counterpart. We investigated $Ddyn$ and $DP2$ ionospheric currents as the mechanisms for such a regional response. As a result, we were able to isolate the magnetic perturbations associated with those ionospheric currents. The combination of these perturbations with planetary response could approximate the regional geomagnetic response.

CRediT authorship contribution statement

Castellanos-Velazco, C. I.: Methodology, Conceptualization, Data analysis, Software, Writing - Original Draft. **Corona-Romero, P.:** Conceptualization, Methodology, Software, Writing - Review & Editing. **González-Esparza, J. A.:** Data revision, Review & Editing. **Caccavari-Garza, A. L.:** Regional magnetic data, Review & Editing. **Sergeeva, M. A.:** Local ionospheric data, Review & Editing.

Declaration of competing interest

The authors declare that they have no known competing financial interests or personal relationships that could have appeared to influence the work reported in this paper.

Data Availability

Data will be made available on request.

Acknowledgments

P. Corona-Romero is grateful for Investigadores por México-CONAHCYT (CONAHCYT Research Fellow) project 1045 Space Weather Service, financed by “Consejo Nacional de Ciencia y Tecnología” (CONAHCYT), which partially supported this work. C.I. Castellanos-Velazco is grateful for “La Beca de Posgrado en México” granted by CONAHCYT. LANCE acknowledges partial financial support from CONHACyT-AEM grant 2017-01-292684, CONAHCyT LN-315829, and PAPIIT IN116023.

This work used data from the Teoloyucan Magnetic Observatory operated by the Magnetic Service of the Geophysics Institute at National and Autonomous University of Mexico (UNAM). Total electron content (TEC) and the geomagnetic indices ΔH and K , the regional counterparts of Dst and K_p indices respectively, are produced by the Mexican Space Weather National Laboratory (LANCE), Geophysics Institute at National and Autonomous University of Mexico (UNAM).

The results presented in this paper rely on K_p and Dst geomagnetic indices calculated by the Helmholtz-Zentrum Potsdam Deutsches GeoForschungsZentrum Adolf-Schmidt-Observatorium and the World Data Center for Geomagnetism, Kyoto, respectively, from data collected at magnetic observatories. We thank the involved national institutes, the INTERMAGNET network and ISGI.

All authors have seen and approved the final version of the manuscript.

References

- Amory-Mazaudier, C., Bolaji, O.S., Doumbia, V., 2017. On the historical origins of the CEJ, DP2, and Ddyn current systems and their roles in the predictions of ionospheric responses to geomagnetic storms at equatorial latitudes. *Journal of Geophysical Research (Space Physics)* 122, 7827–7833. doi:10.1002/2017JA024132.
- Bailey, R.L., Halbedl, T.S., Schattauer, I., Römer, A., Achleitner, G., Beggan, C.D., Wesztergom, V., Egli, R., Leonhardt, R., 2017. Modelling geomagnetically induced currents in midlatitude Central Europe using a thin-sheet approach. *Annales Geophysicae* 35, 751–761. doi:10.5194/angeo-35-751-2017.
- Baumjohann, W., Treumann, R.A., 1999. Basic Space Plasma Physics. Imperial College Press, 57 Shelton Street Covent Garden London WC2H 9HE.
- Blanc, M., Caudal, G., 1985. The spatial distribution of magnetospheric convection electric fields at ionospheric altitudes: a review. II. Theories. *Annales Geophysicae* 3, 27–42.
- Blanc, M., Richmond, A.D., 1980. The ionospheric disturbance dynamo. 85, 1669–1686. doi:10.1029/JA085iA04p01669.
- Bobova, V.P., Vladimirkii, B.M., Pudovkin, M.I., 1985. The presence in the AE index of 160-minute pulsations evidently caused by solar pulsations. *Izvestiya Ordona Trudovogo Krasnogo Znameni Krymskogo Astrofizicheskogo Observatorii* 71, 19–25.
- Carrillo-Vargas, A., Pérez-Enríquez, R., Rodríguez-Martínez, M., López-Montes, R., Casillas-Pérez, G.A., Araujo-Pradere, E.A., 2012. Ionospheric disturbances detected by MEXART. *Advances in Space Research* 49, 1570–1580. doi:10.1016/j.asr.2011.12.017.
- Corona-Romero, P., Sanchez-Garcia, E., Sergeeva, M., Gonzalez-Esparza, J., Cifuentes-Nava, G., Hernandez-Quintero, E., Caccavari, A., Aguilar-Rodriguez, E., Mejía-Ambriz, J., de-la-Luz, V., Gonzalez, L., 2018. Kmex: the mexican geomagnetic k index, in: Proceedings of the II Pan-American Workshop on Geomagnetism, Basouras, Brazil. pp. 96–100.
- Corona-Romero, P., Sergeeva, M., Gonzalez-Esparza, J., Cifuentes-Nava, G., Hernandez-Quintero, E., Caccavari, A., Sanchez-Garcia, E., 2017. Mexican geomagnetic k index , 1–6.
- C.T Russell, J. G. Luhman, R.J.S., 2016. SPACE PHYSICS AN INTRODUCTION. Cambridge university press. University Princting House, Cambridge CB2 (BS, United Kingdom).
- da Silva Barbosa, C., Hartmann, G.A., Pinheiro, K.J., 2015. Numerical modeling of geomagnetically induced currents in a Brazilian transmission line. *Advances in Space Research* 55, 1168–1179. doi:10.1016/j.asr.2014.11.008.
- Denisenko, V.V., Zamai, S.S., Kitaev, A.V., Matveenkov, I.T., Pivovarov, V.G., 1992. System of ionospheric currents excited by a magnetospheric generator in the boundary layer. *Geomagnetism and Aeronomy* 32, 142–145.
- Gjerloev, J.W., 2012. The SuperMAG data processing technique. *Journal of Geophysical Research (Space Physics)* 117, A09213. doi:10.1029/2012JA017683.
- Gonzalez, W.D., Joselyn, J.A., Kamide, Y., Kroehl, H.W., Rostoker, G., Tsurutani, B.T., Vasiliunas, V.M., 1994. What is a geomagnetic storm? 99, 5771–5792. doi:10.1029/93JA02867.
- Gonzalez-Esparza, A., Carrillo, A., Andrade, E., Jeyakumar, S., Ananthakrishnan, S., Praveenkumar, A., Sankarasubramanian, G., Suresh Kumar, S., Sierra, P., Vazquez, S., Perez-Enriquez, R., Kurtz, S., 2005. MEXART Measurements of Radio Sources. Interplanetary Scintillation Array in Mexico, in: AGU Fall Meeting Abstracts, pp. SH51C–1218.
- Gonzalez-Esparza, J.A., De la Luz, V., Corona-Romero, P., Mejia-Ambriz, J.C., Gonzalez, L.X., Sergeeva, M.A., Romero-Hernandez, E., Aguilar-Rodriguez, E., 2017. Mexican space weather service (sciesmex). *Space Weather* 15, 3–11. URL: <https://agupubs.onlinelibrary.wiley.com/doi/abs/10.1002/2016SW001496>, arXiv:<https://agupubs.onlinelibrary.wiley.com/doi/pdf/10.1002/2016SW001496>.
- Hejda, P., Bochníček, J., 2005. Geomagnetically induced pipe-to-soil voltages in the Czech oil pipelines during October–November 2003. *Annales Geophysicae* 23, 3089–3093. doi:10.5194/angeo-23-3089-2005.
- Heppner, J.P., 1972a. Electric Fields in the Magnetosphere, in: Dyer, E.R. (Ed.), Critical Problems of Magnetospheric Physics, p. 107.
- Heppner, J.P., 1972b. Polar-cap electric field distributions related to the interplanetary magnetic field direction. 77, 4877–4887. doi:10.1029/JA077i025p04877.
- Kikuchi, T., Hashimoto, K.K., 2016. Transmission of the electric fields to the low latitude ionosphere in the magnetosphere-ionosphere current circuit. *Geoscience Letters* 3, 4. doi:10.1186/s40562-016-0035-6.
- Knecht, D., B.M., S., 1985. HANDBOOK OF GEOPHYSICS AND THE SPACE ENVIRONMENT, chapter 4, THE GEOMAGNETIC FIELD. ed by A. S. Jursa, Boston: Air Force Geophysics Laborator.
- Le Huy, M., Amory-Mazaudier, C., 2005. Magnetic signature of the ionospheric disturbance dynamo at equatorial latitudes: “ D_{dyn} ”. *Journal of Geophysical Research (Space Physics)* 110, A10301. doi:10.1029/2004JA010578.
- López-Montes, R., Pérez-Enríquez, R., Araujo-Pradere, E.A., 2012. The impact of large solar events on the total electron content of the ionosphere at mid latitudes. *Advances in Space Research* 49, 1167–1179. doi:10.1016/j.asr.2012.01.008.
- Martínez-Bretón L., J., Ortega, B., Hernandez-Quintero, J.E., 2016. Relationship between the minima of the horizontal magnetic component measured in mexico and the dst and sym-h indices for geomagnetic storms with dst -100nt during the descending phase of solar cycle 23. *Geofísica Internacional* 55, 155–164.
- Mayaud, P.N., 1980. Derivation, Meaning, and Use of Geomagnetic Indices. *Geophysical Monograph Series* 22, 607. doi:10.1029/GM022.
- Merline Matamba, T., Habarulema, J.B., Burešová, D., 2016. Midlatitude ionospheric changes to four great geomagnetic storms of solar cycle 23 in Southern and Northern Hemispheres. *Space Weather* 14, 1155–1171. doi:10.1002/2016SW001516.
- Nishida, A., 1966. Formation of plasmapause, or magnetospheric plasma knee, by the combined action of magnetospheric convection and plasma escape from the tail. 71, 5669–5679. doi:10.1029/JZ071i023p05669.

- Nishida, A., 1968a. Coherence of geomagnetic DP 2 fluctuations with interplanetary magnetic variations. 73, 5549–5559. doi:10.1029/JA073i017p05549.
- Nishida, A., 1968b. Geomagnetic D_p 2 fluctuations and associated magnetospheric phenomena. 73, 1795–1803. doi:10.1029/JA073i005p01795.
- Obayashi, T., Nishida, A., 1968. Large-Scale Electric Field in the Magnetosphere. 8, 3–31. doi:10.1007/BF00362569.
- Pérez-Enríquez, R., Kotsarenko, A., 2003. IPS data of the Mexican Array Radio Telescope (MEXART) corrected for ionospheric scintillation and geomagnetic activity, in: EGS - AGU - EUG Joint Assembly, p. 2923.
- Pirjola, R., 2000. Geomagnetically induced currents during magnetic storms. IEEE Transactions on Plasma Science 28, 1867–1873. doi:10.1109/27.902215.
- Rishbeth, H., Garriott, O.K., 1969. Introduction to ionospheric physics.
- Rodriguez-Martinez, M., Perez-Enriquez, R., Carrillo-Vargas, A., Lopez-Montes, R., Araujo-Pradere, E.A., Casillas-Perez, G., Lopez Cruz-Abeyro, J., 2011. Ionospheric Disturbance Effects on IPS signals from MEXART, in: AGU Fall Meeting Abstracts, pp. SH13B–1969.
- Rodriguez-Martinez, M., Perez-Enriquez, R., Carrillo-Vargas, A., Lopez-Montes, R., Araujo-Pradere, E., Casillas, G., Lopez Cruz-Abeyro, J., 2011. Ionospheric disturbance effects on ips signals from mexart. AGU Fall Meeting Abstracts , 1969–.
- Rodriguez-Martinez, M., Pérez-Enríquez, H., Carrillo-Vargas, A., López-Montes, R., Araujo-Pradere, E., Casillas, G., Lopez Cruz-Abeyro, J., 2014. Ionospheric disturbances and their impact on ips using mexart observations. Solar Physics 289. doi:10.1007/s11207-014-0496-8.
- Romero-Hernandez, E., Gonzalez-Esparza, J.A., Rodriguez-Martinez, M., Sergeeva, M.A., Aguilar-Rodriguez, E., Mejia-Ambriz, J.C., De la Luz, V., 2017. Study of ionospheric disturbances over Mexico associated with transient space weather events. Advances in Space Research 60, 1838–1849. doi:10.1016/j.asr.2017.06.042.
- Schrijver, C.J., 2015. Socio-Economic Hazards and Impacts of Space Weather: The Important Range Between Mild and Extreme. Space Weather 13, 524–528. doi:10.1002/2015SW001252, arXiv:1507.08730.
- Sergeeva, M.A., Gonzalez-Esparza, J.A., Blagoveshchensky, D.V., Maltseva, O.A., Chernov, A.G., Corona-Romero, P., De la Luz, V., Mejia-Ambriz, J.C., Gonzalez, L.X., Romero-Hernandez, E., Rodriguez-Martinez, M., Aguilar-Rodriguez, E., Andrade, E., Villanueva, P., Gatica-Acevedo, V.J., 2019. First observations of oblique ionospheric sounding chirp signal in Mexico. Results in Physics 12, 1002–1003. doi:10.1016/j.rinp.2018.12.077.
- Sergeeva, M.A., Maltseva, O.A., Gonzalez-Esparza, J.A., De la Luz, V., Corona-Romero, P., 2017. Features of TEC behaviour over the low-latitude North-American region during the period of medium solar activity. Advances in Space Research 60, 1594–1605. doi:10.1016/j.asr.2017.06.021.
- van de Kamp, M., 2013. Harmonic quiet-day curves as magnetometer baselines for ionospheric current analyses. Geoscientific Instrumentation, Methods and Data Systems 2, 289–304. doi:10.5194/gi-2-289-2013.
- Vodyannikov, V.V., Gordienko, G.I., Nechaev, S.A., Sokolova, O.I., Khomutov, S.Y., Yakovets, A.F., 2006. Geomagnetically induced currents in power lines according to data on geomagnetic variations. Geomagnetism and Aeronomy 46, 809–813. doi:10.1134/S0016793206060168.
- Wei, Y., Zhao, B., Li, G., Wan, W., 2015. Electric field penetration into Earth's ionosphere: a brief review for 2000–2013. Science Bulletin 60, 748–761. doi:10.1007/s11434-015-0749-4.
- Younas, W., Amory-Mazaudier, C., Khan, M., Fleury, R., 2020. Ionospheric and Magnetic Signatures of a Space Weather Event on 25–29 August 2018: CME and HSSWs. Journal of Geophysical Research (Space Physics) 125, e27981. doi:10.1029/2020JA027981.
- Zaka, K.Z., Kobea, A.T., Assamoi, P., Obrou, O.K., Doumbia, V., Boka, K., Adohi, B.J.P., Mene, N.M., 2009. Latitudinal profile of the ionospheric disturbance dynamo magnetic signature: comparison with the DP2 magnetic disturbance. Annales Geophysicae 27, 3523–3536. doi:10.5194/angeo-27-3523-2009.

5. Appendix

Geomagnetic local response associated with geomagnetic storms

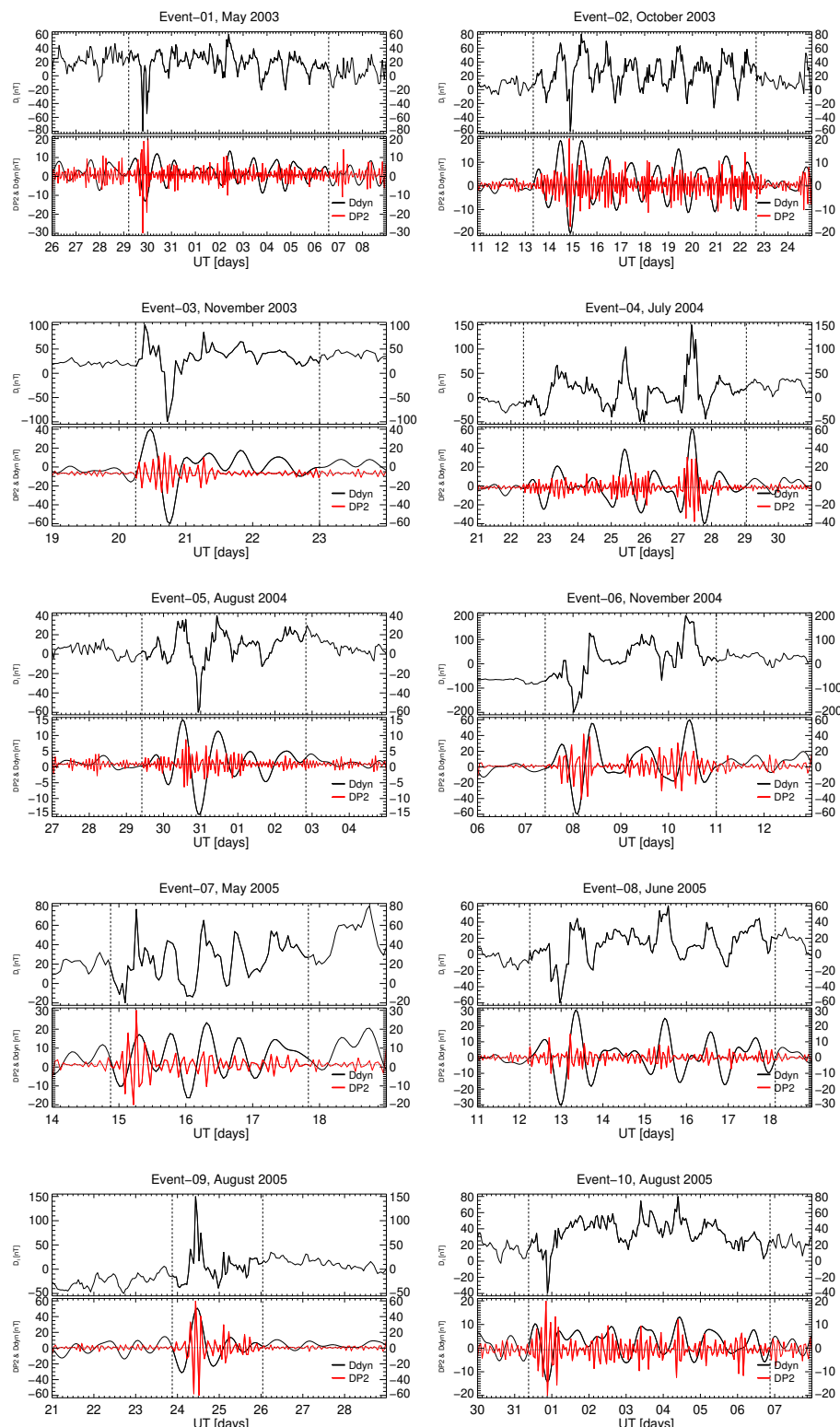


Figure 6: Ionospheric Magnetic Disturbance contribution (top panels) and the isolated Ddyn and DP2 geomagnetic contribution (bottom panels).

1
2
3
4
5
6
7
8
9
10
11
12
13
14
15
16
17
18
19
20
21
22
23
24
25
26
27
28
29
30
31
32
33
34
35
36
37
38
39
40
41
42
43
44
45
46
47
48
49
50
51
52
53
54
55
56
57
58
59
60
61
62
63
64
65

Geomagnetic local response associated with geomagnetic storms

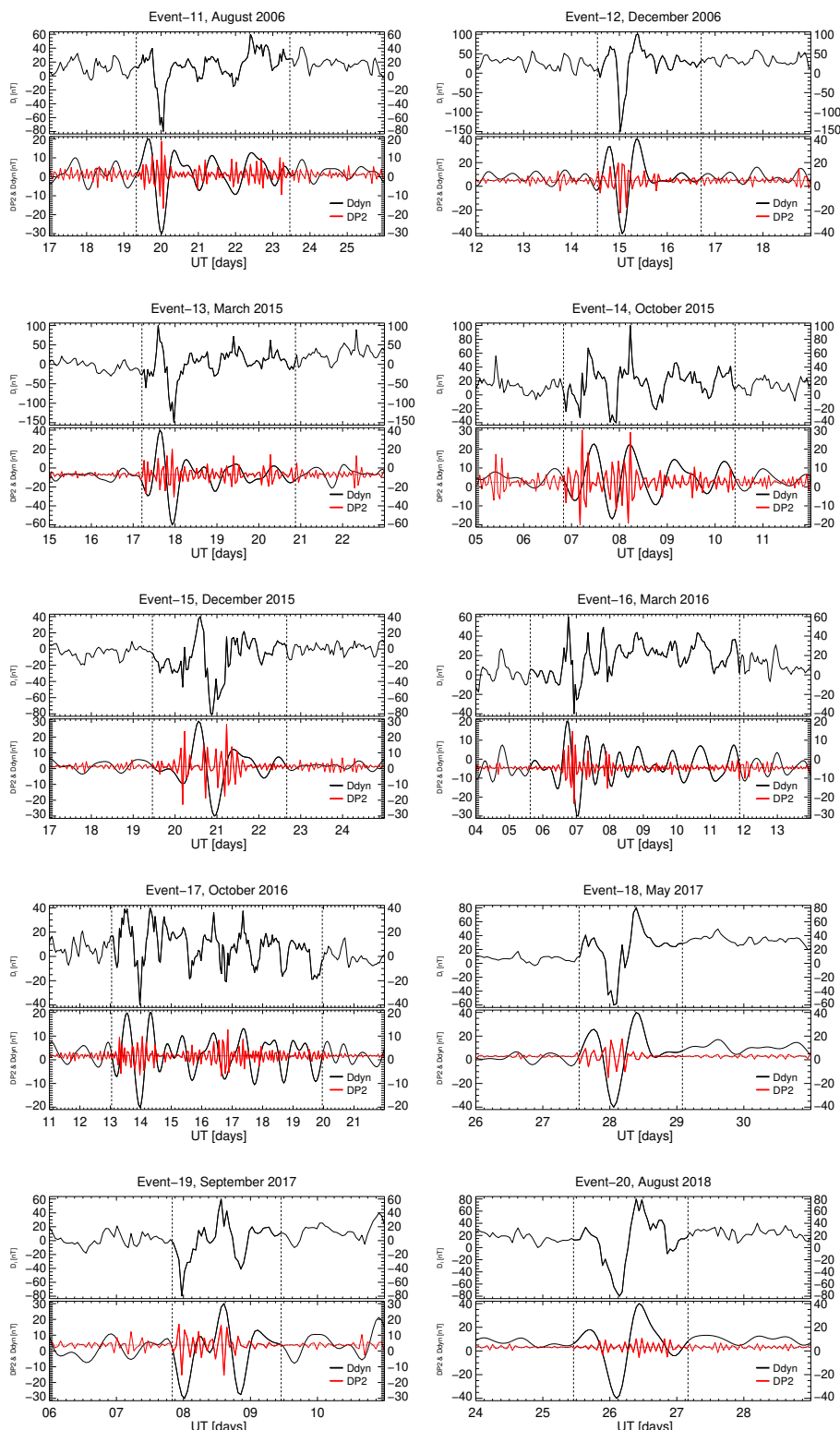


Figure 7: Ionospheric Magnetic Disturbance contribution (top panels) and the isolated D_{dyn} and DP_2 geomagnetic contribution (bottom panels).

Geomagnetic local response associated with geomagnetic storms

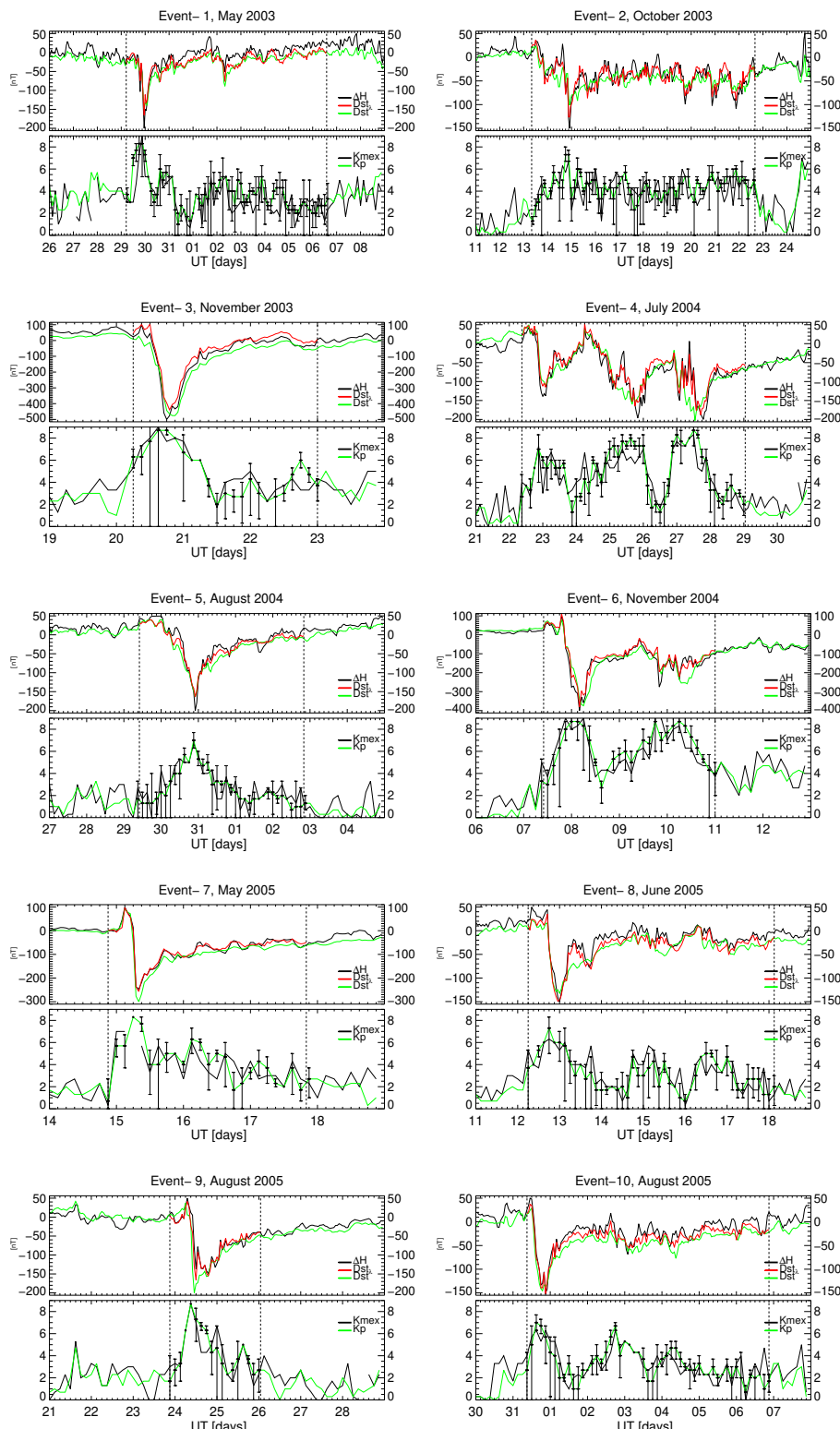


Figure 8: Top: Approximation of ΔH (red line). Bottom: Approximation of K local with a ΔK affection range (error bars).

Geomagnetic local response associated with geomagnetic storms

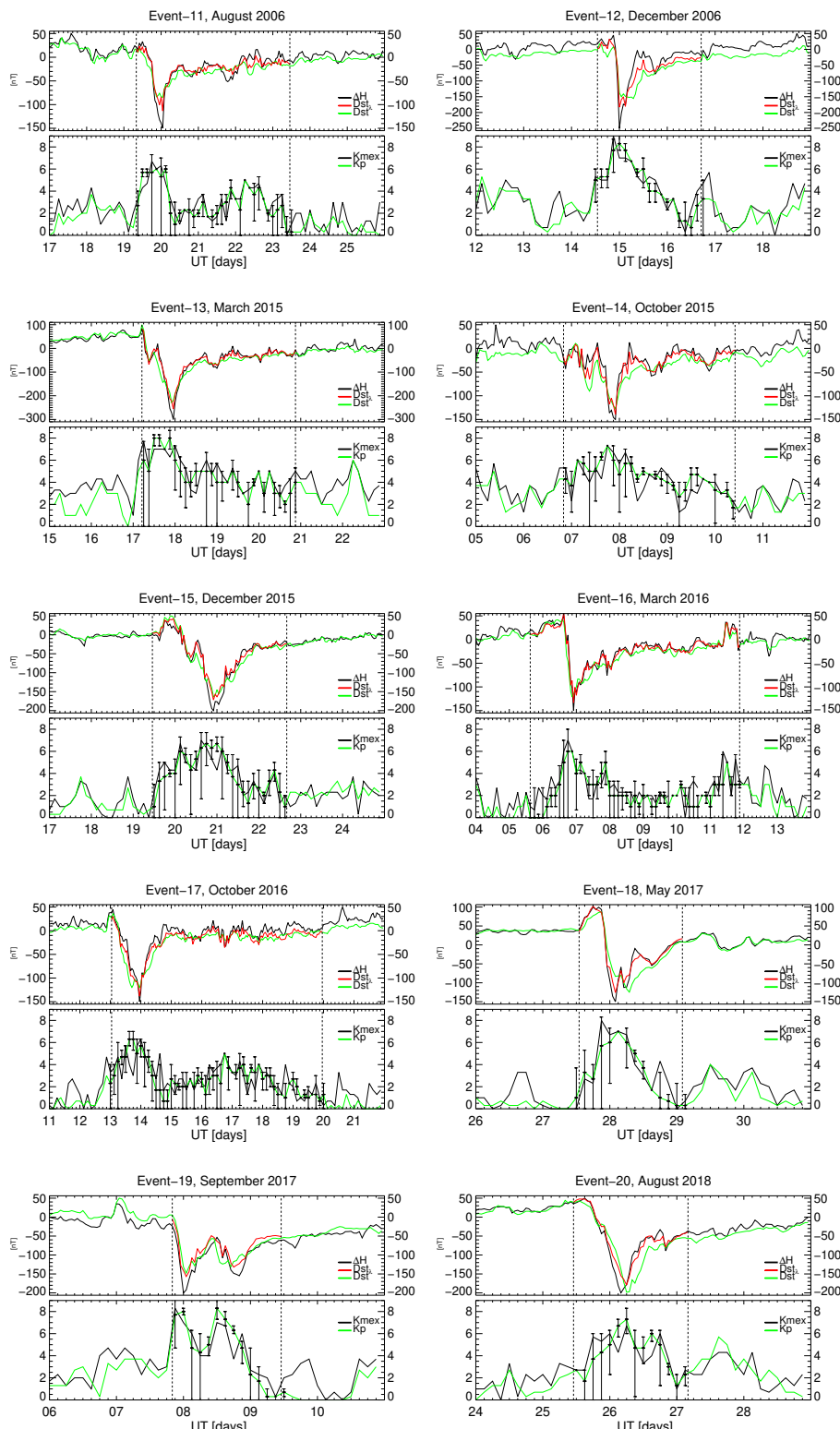


Figure 9: Top: Approximation of ΔH (red line). Bottom: Approximation of K local with a ΔK affection range (error bars).

We certify that all authors have read and approved the final version of the manuscript being submitted. We also warrant that the article is the authors' original work, hasn't received prior publication and isn't under consideration for publication elsewhere.

Declaration of Interest Statement

The authors declare that they have no known competing financial interests or personal relationships that could have appeared to influence the work reported in this paper.